Supporting Information for Publication

An APXPS Probe of Cu/Pd Bimetallic Catalysts Surface Chemistry of CO_2 Toward CO in the Presence of H_2O and H_2

Maxime Leclerc[†,‡], Ane Etxebarria[‡,1,2], Yifan Ye[‡,3], Ethan J. Crumlin[‡,3]*, Gessie M. Brisard[†]*

† Department of Chemistry, University of Sherbrooke, Sherbrooke, QC J1K 2R1, Canada;
‡ Advanced Light Source, Lawrence Berkeley National Laboratory, 1 Cyclotron Road, Berkeley, CA 94720, United State;
1 Centre for Cooperative Research on Alternative Energies (CIC energiGUNE), Basque Research and Technology Alliance (BRTA), Alava Technology Park, Albert Einstein 48, 01510 Vitoria-Gasteiz, Spain;
2 Departamento de Física de la Materia Condensada, Facultad de Ciencia y Tecnología, Universidad del País Vasco, UPV/EHU, P.O. Box 644, 48080 Bilbao, Spain;
3 Chemical Sciences Division, Lawrence Berkeley National Laboratory, Berkeley, CA 94720, United State

Index **Page**

Surface cleaning procedure:

The surfaces were cleaned in the XPS chamber using a repetitive cycle of oxidation and reduction. Cu 3p, O 1s and C 1s signals were followed continuously during the cleaning at 670 eV. Examples of spectra from the cleaning process are shown in the figure SI-4. To begin the cycle, 200 mTorr of $O_{2(g)}$ (Praxair, 99.999%) was introduced in the chamber. The temperature was increased and maintained at 220 °C to oxidize the adventitious carbon and desorb the oxidized carbon species from the surface. These two processes remove nearly all trace of carbon from the surfaces. 1 ML Cu/Pd and Cu surfaces both show oxidation of copper during the increase of temperature. The oxidation is visible on both the Cu 3p and the O 1s spectra. Once the C 1s signal is small and shows no further carbon removal, the temperature is decreased to room temperature and oxygen is removed. The samples are then exposed to 25 mTorr of $H_{2(g)}$ to reduce the copper on the 1 ML Cu/Pd surface. The CuO/Cu surface is not reduced and remains partially oxidized. The introduction of $H_{2(g)}$ in the chamber at a low temperature causes some adventitious carbon species or precursor to be produced in the chamber and deposited on the surface. The oxidation/reduction cycles were repeated until the adventitious carbon deposition during the reduction step was minimized to a stable amount from one cycle to the next. 2 to 5 repetitions were usually necessary to reach the cleanest condition.

Calculation for the photoelectron attenuation model (PAM):

Application of the PAM to the Cu/Pd catalyst: The PAM approximates the Cu/Pd catalyst as composed of 3 perfectly homogenous and flat layer with variable thickness disposed one on the other. The deepest is the metallic palladium substrate, which is covered by the second is the layer of metallic copper, which is itself covered by the surface layer regrouping all the carbon species. Oxygen based species which not contain carbon as hydroxyls and water are neglected in our model. We chose to approximate the layer of carbon species to a homogenous composition. The intensity of each layer follows these proportionalities:

$$I_{Pd} \sim N_{Pd} * \beta_{Pd} * \alpha_{\frac{Pd}{Cu}} * \alpha_{\frac{Pd}{C}} \qquad \text{Eq. SI-1}$$

$$I_{Cu} \sim N_{Cu} * \beta_{Cu} * \alpha_{Pd/C} \quad \text{Eq. SI-2}$$

$$I_{C,i} \sim N_{C,i} * \beta_{C} \quad \text{Eq. SI-3}$$

with I_A : the intensity of the signal of the layer A, measured from the data;

$I_{C,i}$: the intensity of the signal of a carbon specie i, measured form the convolution of the data; β_A : the factor standing for the amount of signal produced by the layer A itself, calculated in Eq. SI-4;

$\alpha_{A/B}$: the attenuation factor of the signal of the layer A by the overlayer B, calculated in Eq. SI-5;

N_A : the normalisation factor of for the layer A, calculated in Eq. SI-6;

$N_{C,i}$: the normalisation factor of for the carbon specie I, calculated in Eq. SI-7.

The factors β and α and N are expressed as:

$$\beta_A = \left(1 - \exp\left(-\frac{t_A}{\lambda_{A/A}}\right)\right) \quad \text{Eq. SI-4}$$

$$\alpha_{A/B} = \exp\left(-\frac{t_B}{\lambda_{A/B}}\right) \quad \text{Eq. SI-5}$$

$$N_A = c_A * \sigma_A * \lambda_{A/A} * B_A \quad \text{Eq. SI-6}$$

$$N_{C,i} = c_i * \sigma_C * \lambda_{C/C} * B_C \quad \text{Eq. SI-7}$$

with t_A and t_B : the thickness of the layer A and B, which represent the unknown variables;

$\lambda_{A/A}$ and $\lambda_{A/B}$ the main free path of the photoelectrons emitted by the atom A crossing respectively the layer A itself and the overlayer B, calculated from Eq. SI5-8; c_A : the concentration of the atom A in the layer A per volume, taken as a reference value;

c_i : the concentration of the carbon specie i in the layer of carbon specie by volume, calculated from Eq. SI5-9; σ_A : the cross section of the atom A excited by the X-ray with a specific photon energy, taken as a reference value;

B_A : the intensity of the X-ray beam used to probe the signal of the atom A, known from the experimentation.

The mean free path $\lambda_{A/B}$ (in nm) is evaluated by the empiric relation taken from Walton *et al.*[1]:

$$\lambda_{A/B} = \frac{\left(0{,}73 + 0{,}0095\ {KE_A}^{0{,}872}\right)}{{Z_B}^{0{,}3}} \qquad \text{Eq. SI-8}$$

with KE_A : the kinetic energy of the photoelectrons emitted by the atom A, known from the experimentation;

Z_B : the average atomic number of the atoms in the layer B, taken as a reference value for the Cu and Pd layers, and calculated for the C layer in Eq. SI-10.

The variable Z_C and c_i dependent on the composition of the layer of carbon species are expressed as:

$$c_i = \frac{I_{C,i}}{\sum_i (V_i * I_{C,i})} \qquad \text{Eq. SI-9}$$

$$Z_C = \frac{\sum_i (I_{C,i} * Z_i * n_i)}{\sum_i (I_{C,i} * n_i)} \qquad \text{Eq. SI-10}$$

with V_i : the molecular volume of the carbon species I, taken as a reference value;

Z_i : the average atomic number of the carbon species I, taken as a reference value;

n_i : the number of atoms in the carbon specie, taken as a reference value.

<u>Mathematical derivation of the Cu content of the Cu/Pd surface</u>: The thickness of the copper monolayer can be obtained from the following division:

$$\frac{I_{Cu}}{I_{Pd}} = \frac{N_{Cu} * \beta_{Cu} * \alpha_{Cu/C}}{N_{Pd} * \beta_{Pd} * \alpha_{Pd/Cu} * \alpha_{Pd/C}} = \frac{N_{Cu} * \alpha_{Cu/C}}{N_{Pd} * \alpha_{Pd/C}} * \frac{\left(1 - \exp\left(-\frac{t_{Cu}}{\lambda_{Cu/Cu}}\right)\right)}{\left(1 - \exp\left(-\frac{t_{Pd}}{\lambda_{Pd/Pd}}\right)\right) * \exp\left(-\frac{t_{Cu}}{\lambda_{Pd/Cu}}\right)} \qquad \text{Eq. SI-11}$$

We approximate $\exp\left(-\frac{t_{Pd}}{\lambda_{Pd/Pd}}\right) = 0$ because the thickness of the palladium substrate t_{Pd} is multiple order of magnitude larger than the mean free path $\lambda_{Pd/Pd}$. The rearrangement of the Eq. SI-11 provides the equation to calculate the thickness of the copper layer t_{Cu}:

$$t_{Cu} = \lambda_{Pd/\,Cu} * \ln\left(\frac{I_{Cu} * N_{Pd} * \alpha_{Pd/C}}{I_{Pd} * N_{Cu} * \alpha_{Cu/C}} + \exp\left(t_{Cu} * \left(\frac{1}{\lambda_{Pd/Cu}} - \frac{1}{\lambda_{Cu/Cu}}\right)\right)\right) \qquad \text{Eq. SI-12}$$

The thickness of the carbon layer t_C can be obtained by the following division:

$$\frac{I_{C,i}}{I_{Cu}} = \frac{N_{C,i} * \beta_C}{N_{Cu} * \beta_{Cu} * \alpha_{Cu/C}} = \frac{N_{C,i}}{N_{Cu}} * \frac{\left(1 - \exp\left(-\frac{t_C}{\lambda_{C/C}}\right)\right)}{\left(1 - \exp\left(-\frac{t_{Cu}}{\lambda_{Cu/Cu}}\right)\right) * \exp\left(-\frac{t_C}{\lambda_{Cu/C}}\right)} \qquad \text{Eq. SI-13}$$

The rearrangement of the Eq. SI-13 gives expression of the total thickness of the carbon layer t_C:

$$t_C = \lambda_{Cu/\,C} * \ln\left(\frac{N_{Cu} * \left(1 - \exp\left(-\frac{t_{Cu}}{\lambda_{Cu/Cu}}\right)\right) * \sum_i (V_i * I_i)}{I_{Cu} * \sigma_C * \lambda_{C/C} * B_C} + \exp\left(t_C * \left(\frac{1}{\lambda_{Cu/C}} - \frac{1}{\lambda_{C/C}}\right)\right)\right) \qquad \text{Eq. SI-14}$$

The calculus of t_{Cu} and t_C in Eq. SI-12 and Eq. SI-14 calls for the values of t_{Cu} and t_C. The calculation is operated at first with the approximations the factors $\exp\left(t_{Cu} * \left(\frac{1}{\lambda_{Pd/Cu}} - \frac{1}{\lambda_{Cu/Cu}}\right)\right) = 1$ in Eq. SI-12 and $\exp\left(t_C * \left(\frac{1}{\lambda_{Cu/C}} - \frac{1}{\lambda_{C/C}}\right)\right) = 1$ in Eq. SI-14. This provides with approximate first values of t_{Cu} and t_C. These values are reintroduced into the Eq. SI-12 and Eq. SI-14 to provide more accurate values of t_{Cu} and t_C. This reintroduction of the of the newly calculated t_{Cu} and t_C into Eq. SI-12 and Eq. SI-14 is iterated until the result of the calculus converge. The convergence value of t_{Cu} and t_C are kept.

Finally, the coverage of the monolayer of copper θ_{Cu} is calculated convert from the final thickness of the copper layer by using the following equation.

$$\theta_{Cu} = t_{Cu}/d_{Cu} \qquad \text{Eq. SI-15}$$

with d_{Cu} : the effective thickness of a complete monolayer of copper atom, taken as a reference value.

Normalisation of the C 1s signal:

To compensate the attenuation of the signal, which varies with the nature and the pressure of the gases in the main chamber during the experiment, the intensity of the C 1s signal has been normalized. The point of reference for the normalisation is the metallic background from which the signal is attenuated similarly to the C 1s signal. This signal is composed of Cu 3p and of Pd 3d, collected at high photon energy (respectively 670 eV and 660 eV) to increase the signal. Both signal form Cu 3p and of Pd 3d are corrected for their difference of incident beam intensity, of cross section and of mean free path of the emitted photoelectrons. The normalised intensity $I_{N\,C\,1s}$ is obtained by the following equation:

$$I_{N\,C\,1s} = \frac{I_{C\,1s}}{\frac{I_{Pd\,3d}}{\lambda_{Pd\,3d} * \sigma_{Pd\,3d} * B_{Pd\,3d}} + \frac{I_{Cu\,3p}}{\lambda_{Cu\,3p} * \sigma_{Cu\,3p} * B_{Cu\,3p}}} \qquad \text{Eq. SI-16}$$

With $I_{C\,1s}$: the intensity of the C 1s signal, measured experimentally;

$I_{Cu\,3p}$: the signal of the Cu 3p peaks collected at 670 eV, measured experimentally;

$I_{Pd\,3d}$: the signal of the Cu 3p peaks collected at 660 eV, measured experimentally;

B : beam intensity (in A), known from the experimentation;

σ : cross section (in Barn), taken as a reference value from Yeh and Linday[2];

λ : mean free path of the emitted photoelectrons (in m), calculated from Eq. SI5-8.

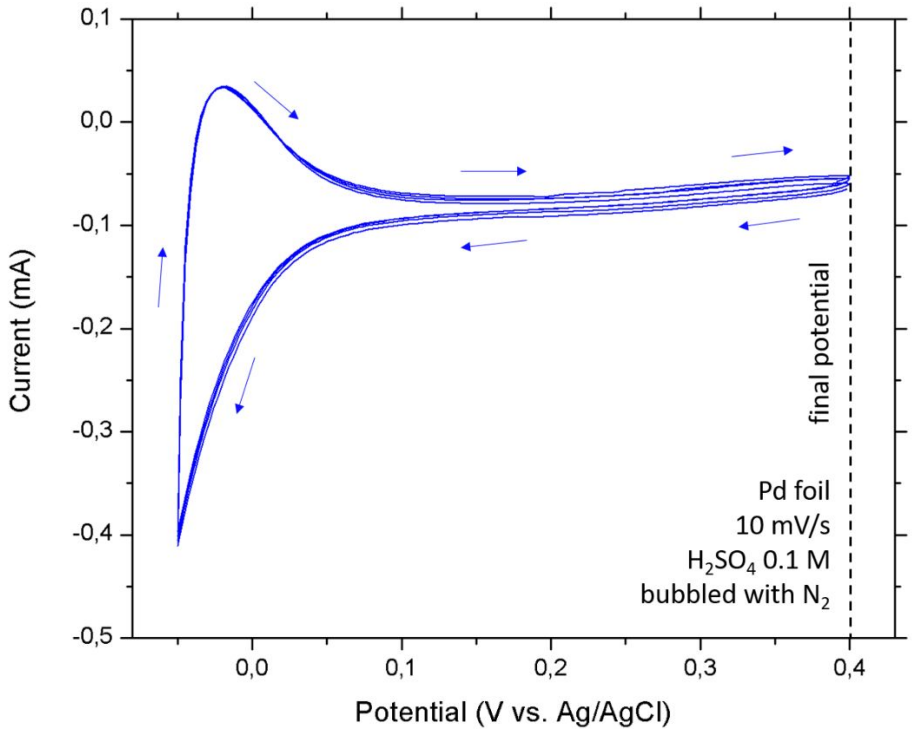

Figure SI-1 : Preparation of the Pd surface by cyclic voltammetry. The current due to $O_{2(aq.)}$ reduction is estimated to -0,08 mA.

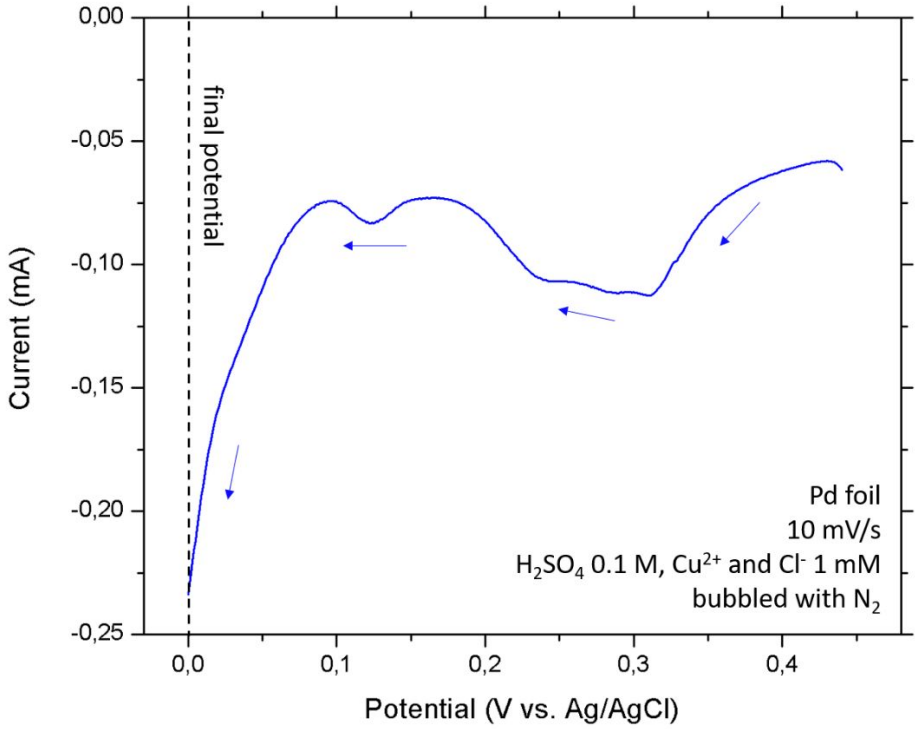

Figure SI-2 : Preparation of the Cu/Pd surface by cathodic sweep. The current due to $O_{2(aq.)}$ reduction is estimated to -0,06 mA.

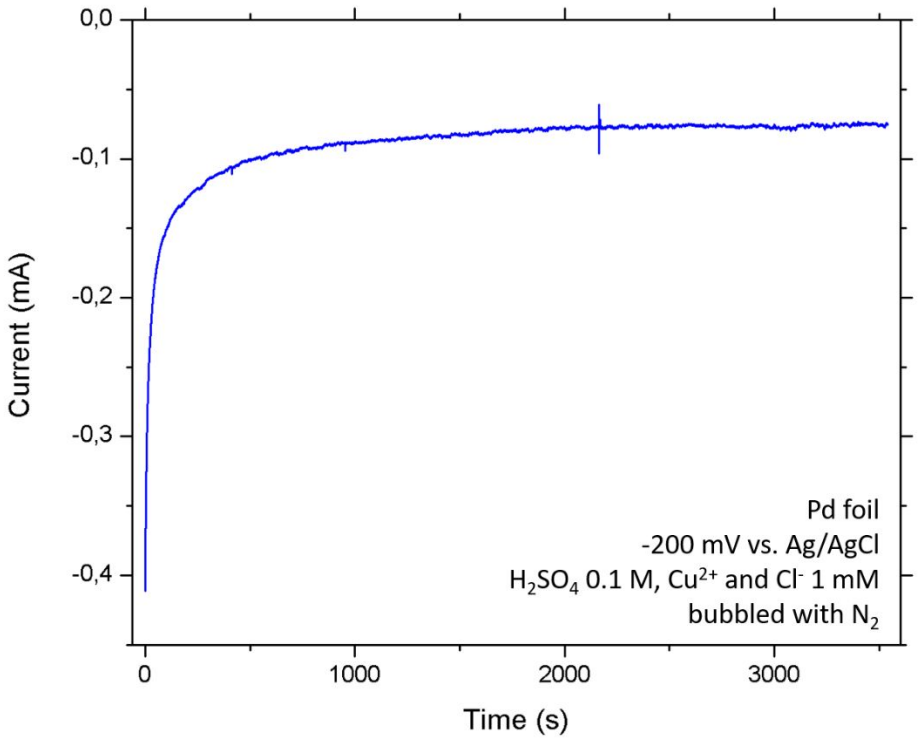

Figure SI-3 : Preparation of the CuO/Cu surface by chronoamperometry. The current due to $O_{2(aq.)}$ reduction is estimated to -0,07 mA.

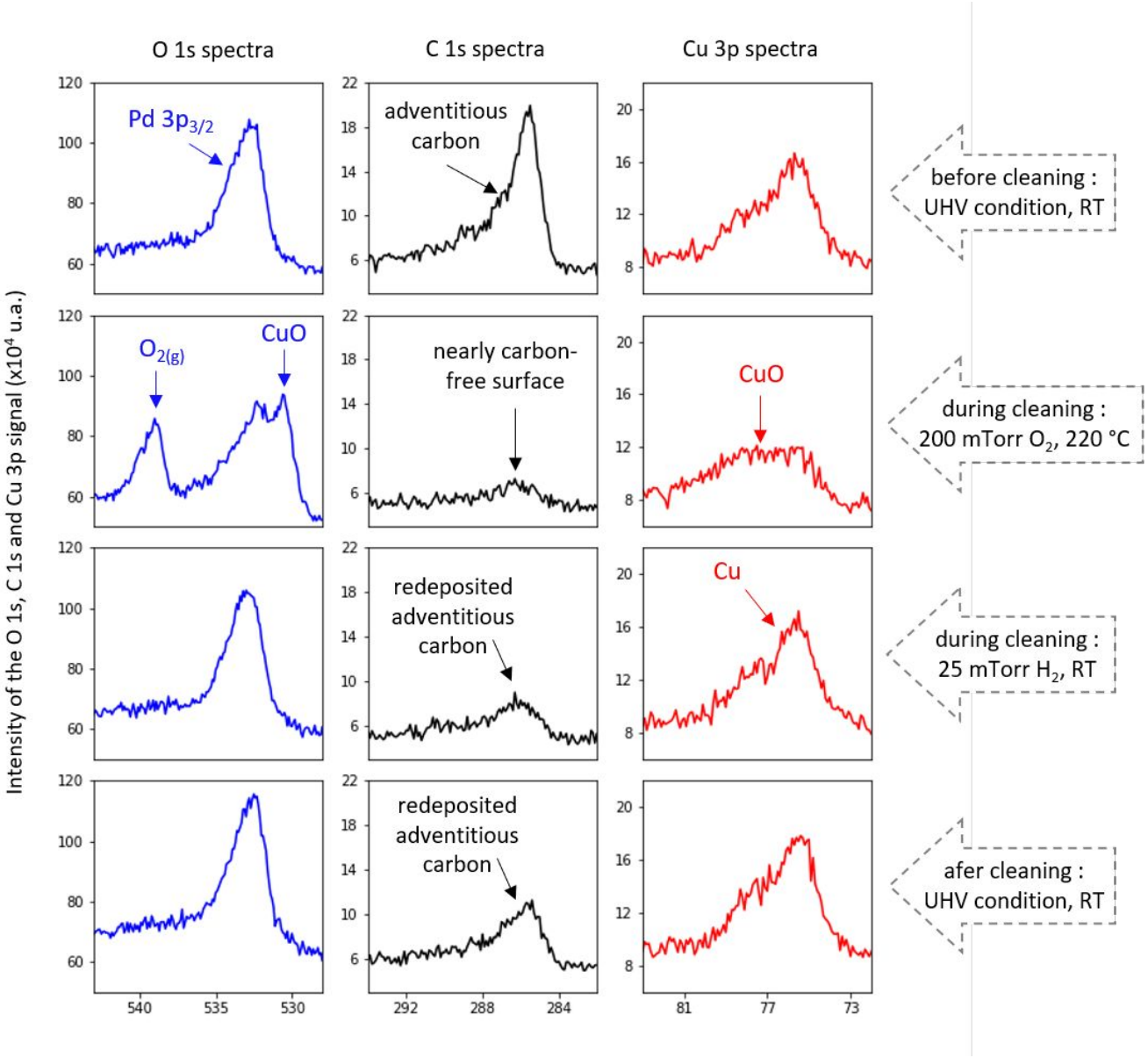

Figure SI-4 : Cleaning process of the Cu/Pd surface. The O 1s (left column), C 1s (middle column) and Cu 3p (right column) spectra have been collected as function of time with a photon energy of 670 eV. The rows of spectra represent the successive step of the cleaning process.

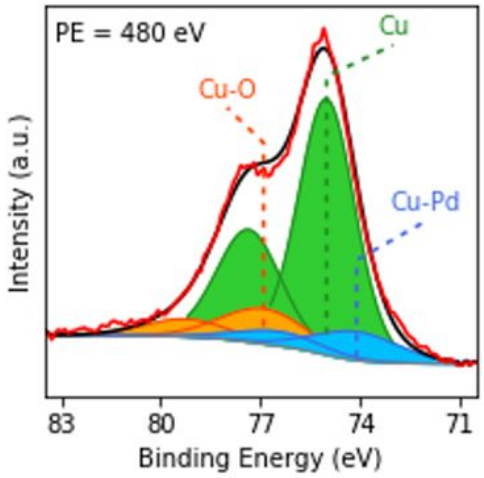

Figure SI-5: Cu 3p spectrum from a non-oxidized Cu surface (correspond to the CuO/Cu surface before the oxidative cleaning process). The metallic Cu peaks (green) can be identified clearly on this spectrum. The Cu-O (orange) and Cu-Pd (blue) species also appear.

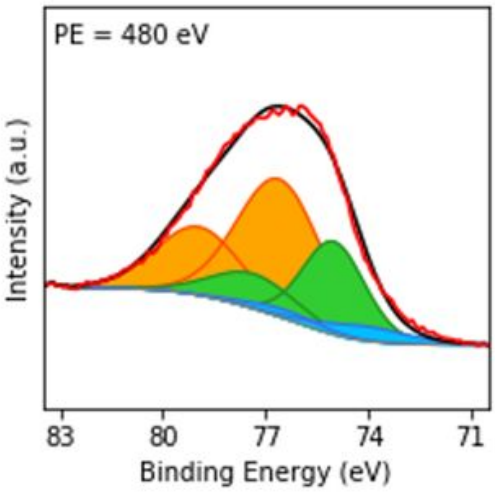

Figure SI-6: Cu 3p spectrum from an oxidized Cu surface (correspond to the CuO/Cu surface after the oxidative cleaning process). The oxidized Cu-O peaks (orange) can be identified clearly on this spectrum. The Cu (green) and Cu-Pd (blue) species also appear.

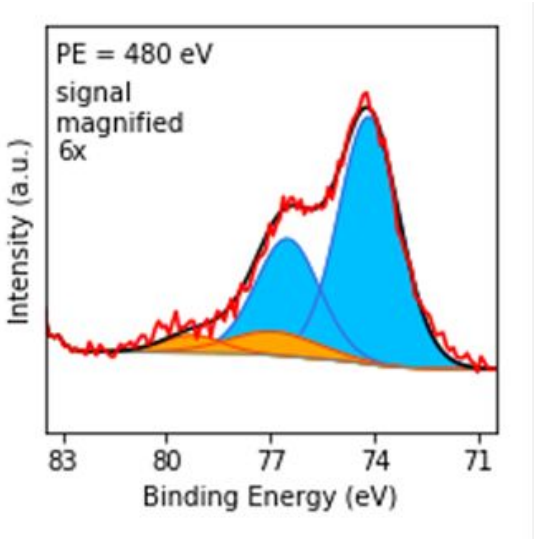

Figure SI-7: Cu 3p spectrum from low content (< 0.4 ML) Cu deposition on a Pd substrate. The sample was prepared by UPD deposition with a methodology similar to the Cu/Pd surface. The Cu-Pd peaks (blue) representing the Cu adatoms directly coordinated by the Pd substrate can be identified clearly on this spectrum. The Cu (green) and Cu-O (orange) species also appear.

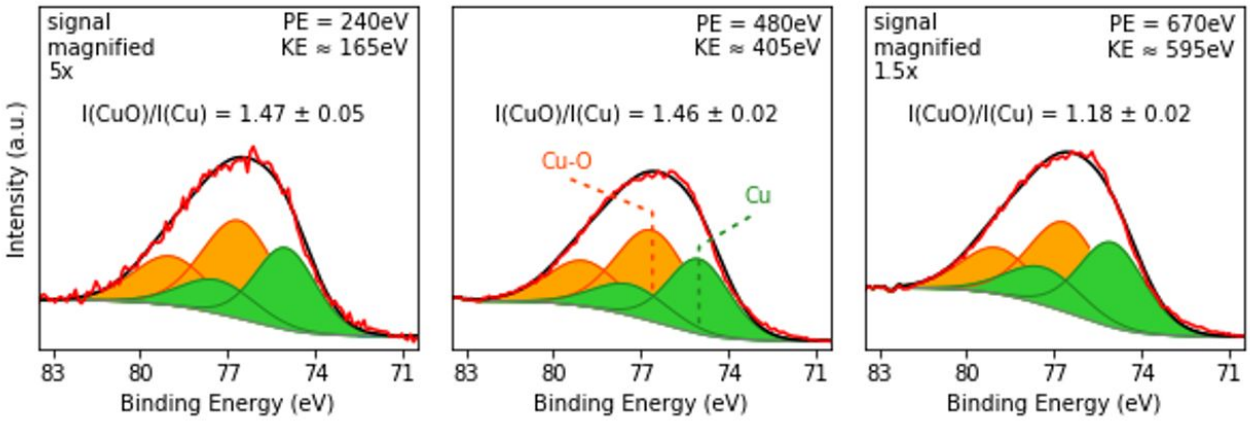

Figure SI-8: Cu 3p spectra of the CuO/Cu surface. The kinetic energy of the X-ray increases from the left spectra to the right spectra. The decrease of the proportion of CuO as the photon energy and probing depth increase implies that the copper oxide is more concentrated at the surface of the Cu material.

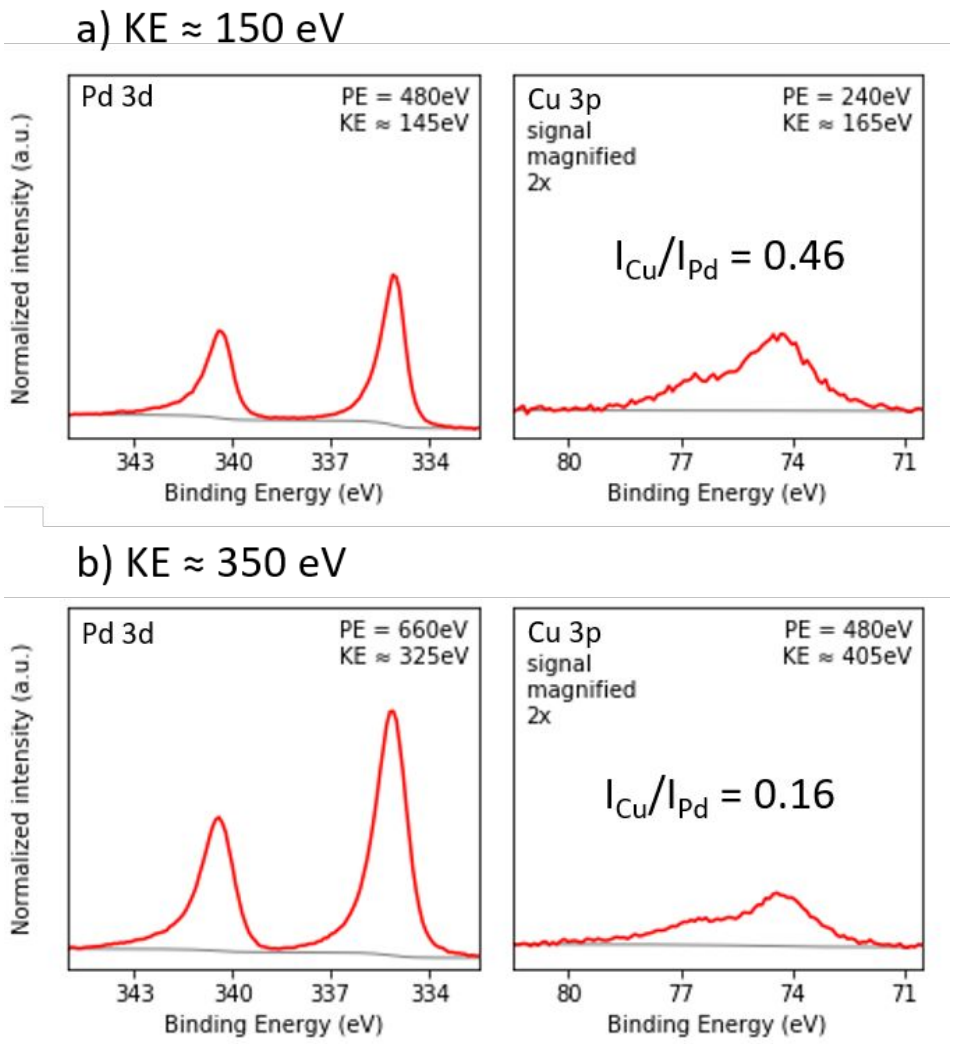

Figure SI-9: Pd 3d and Cu 3p spectra of the Cu/Pd surface with kinetic energy of approximately a) 150 eV and b) 350 eV. Intensity I are normalised with the intensity of the beam B, the cross section σ and the mean free path of the photoelectron λ in the equation $I_N = {}^{I}/_{(B * \sigma * \lambda)}$. The decrease of the proportion of copper in the material as the photon energy increases from a) to b) implies that the copper is concentrated at the surface of the Cu/Pd material.

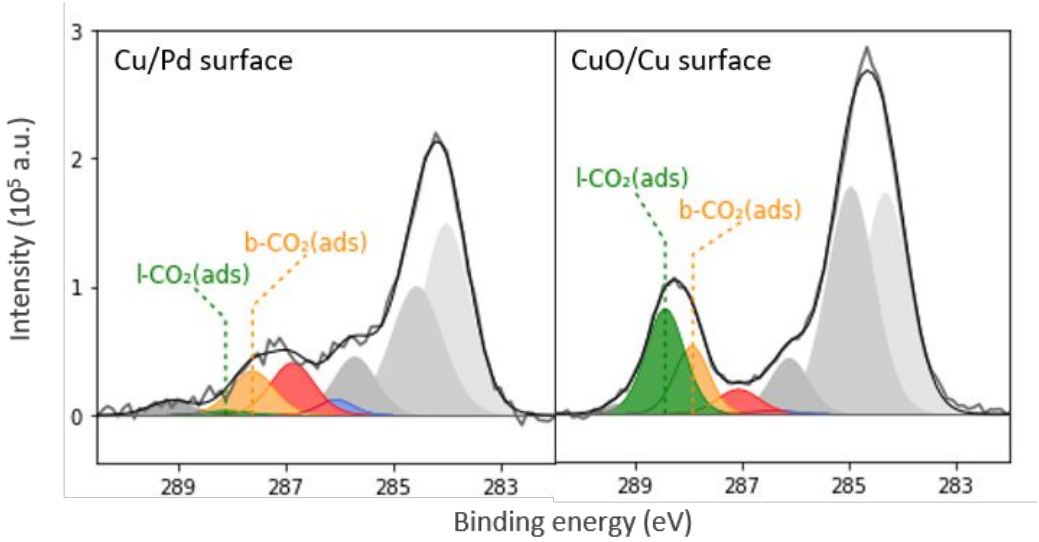

Figure SI-10: C 1s spectra of the CuO/Cu and the Cu/Pd surfaces exposed to 200 mTorr $CO_{2(g)}$ and 50 mTorr of $H_2O_{(g)}$. The l-$CO_{2(ads)}$ (green) and the b-$CO_{2(ads)}$ (yellow) species can be identified clearly on this spectrum. The COOH (red) and the $CO_{(ads)}$ (blue) species also appear.

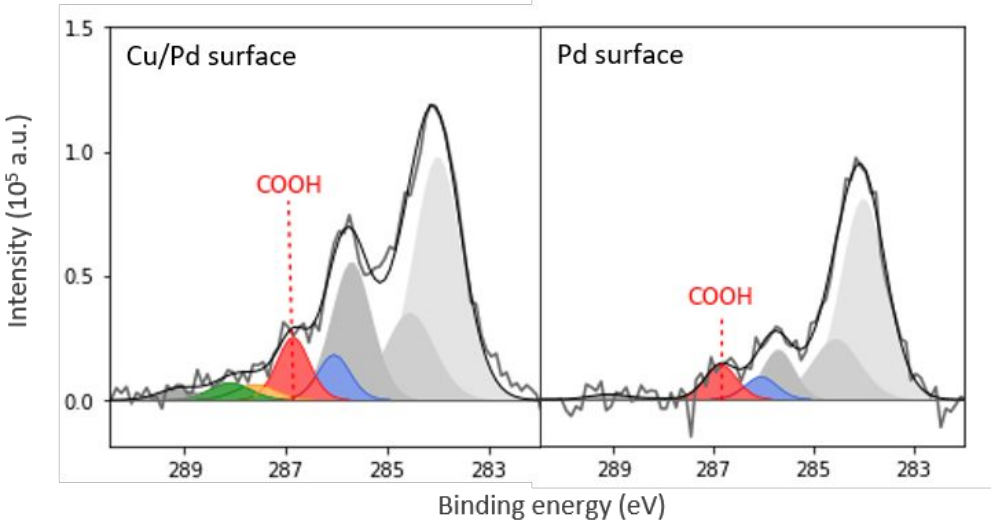

Figure SI-11: C 1s spectra showing the carbon species present on the Cu/Pd and the Pd surfaces exposed to 200 mTorr $CO_{2(g)}$. The COOH (red) species can be identified clearly on this spectrum. The l-$CO_{2(ads)}$ (green), the b-$CO_{2(ads)}$ (yellow) and the $CO_{(ads)}$ (blue) species also appear.

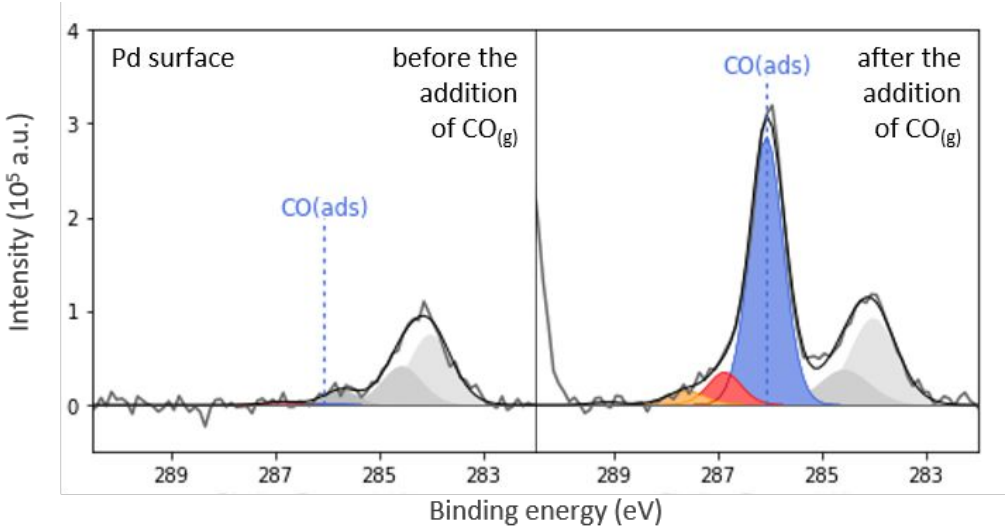

Figure SI-12: C 1s spectra collected on the Pd surface upon the addition of 200 mTorr $CO_{(g)}$. The $CO_{(ads)}$ (blue) species can be identified clearly on this spectrum. The b-$CO_{2(ads)}$ (yellow) and the COOH (red) species also appear.

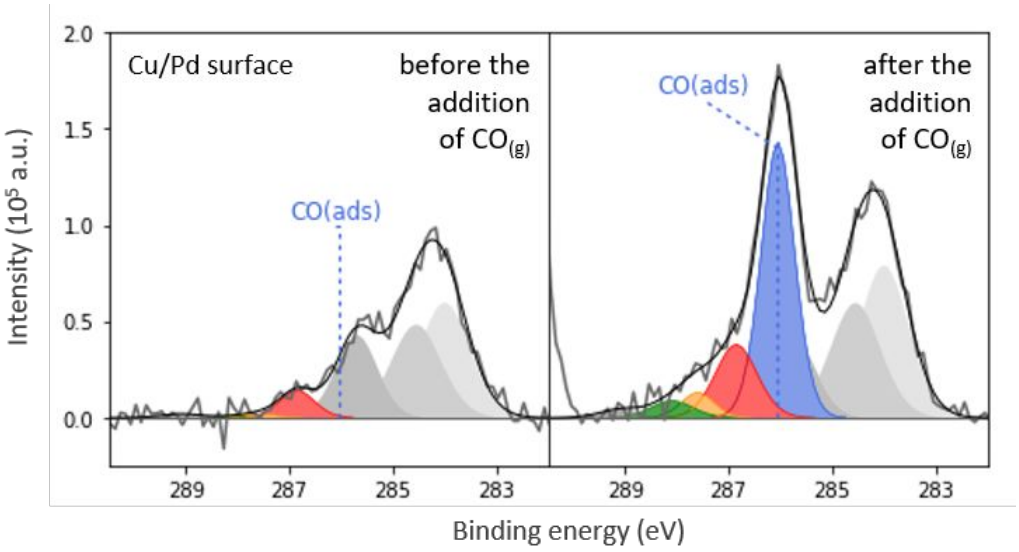

Figure SI-13: C 1s spectra collected on the Cu/Pd surface upon the addition of 200 mTorr $CO_{(g)}$. The $CO_{(ads)}$ (blue) species can be identified clearly on this spectrum. The l-$CO_{2(ads)}$ (green), the b-$CO_{2(ads)}$ (yellow) and the COOH (red) species also appear.

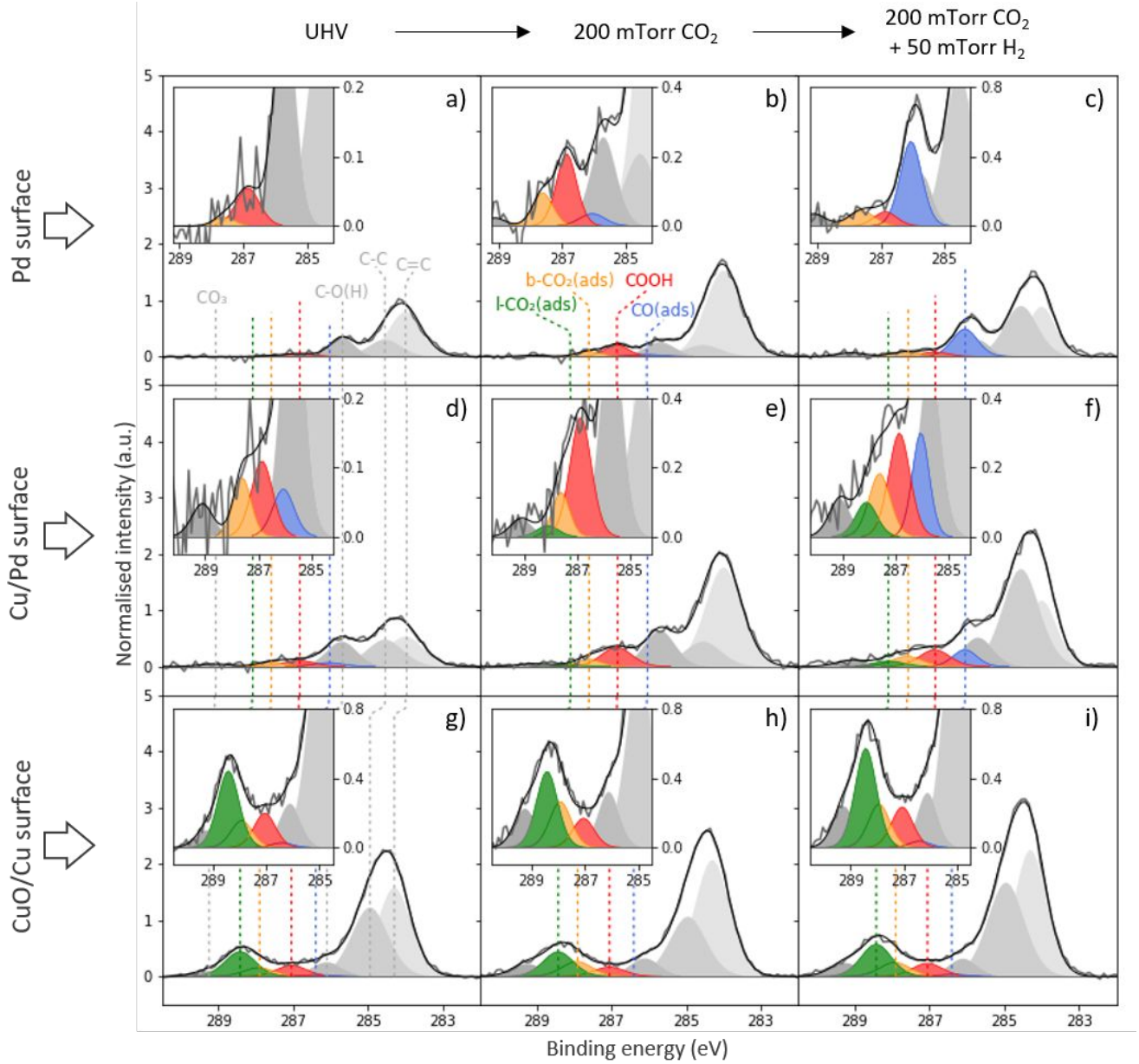

Figure SI-14: C 1s spectra measured at the Pd (a, b and c), Cu/Pd (d, e and f) and CuO/Cu (g, h and i) surfaces during the first run of addition of gas. Spectra are initially collected in UHV conditions (a, d and g) before the addition of 200 mTorr CO_2 (b, e and h) and 50 mTorr H_2 (c, f and i). The species of interest are l-$CO_{2(ads)}$ (green), b-$CO_{2(ads)}$ (yellow), COOH (red) and $CO_{(ads)}$ (blue).

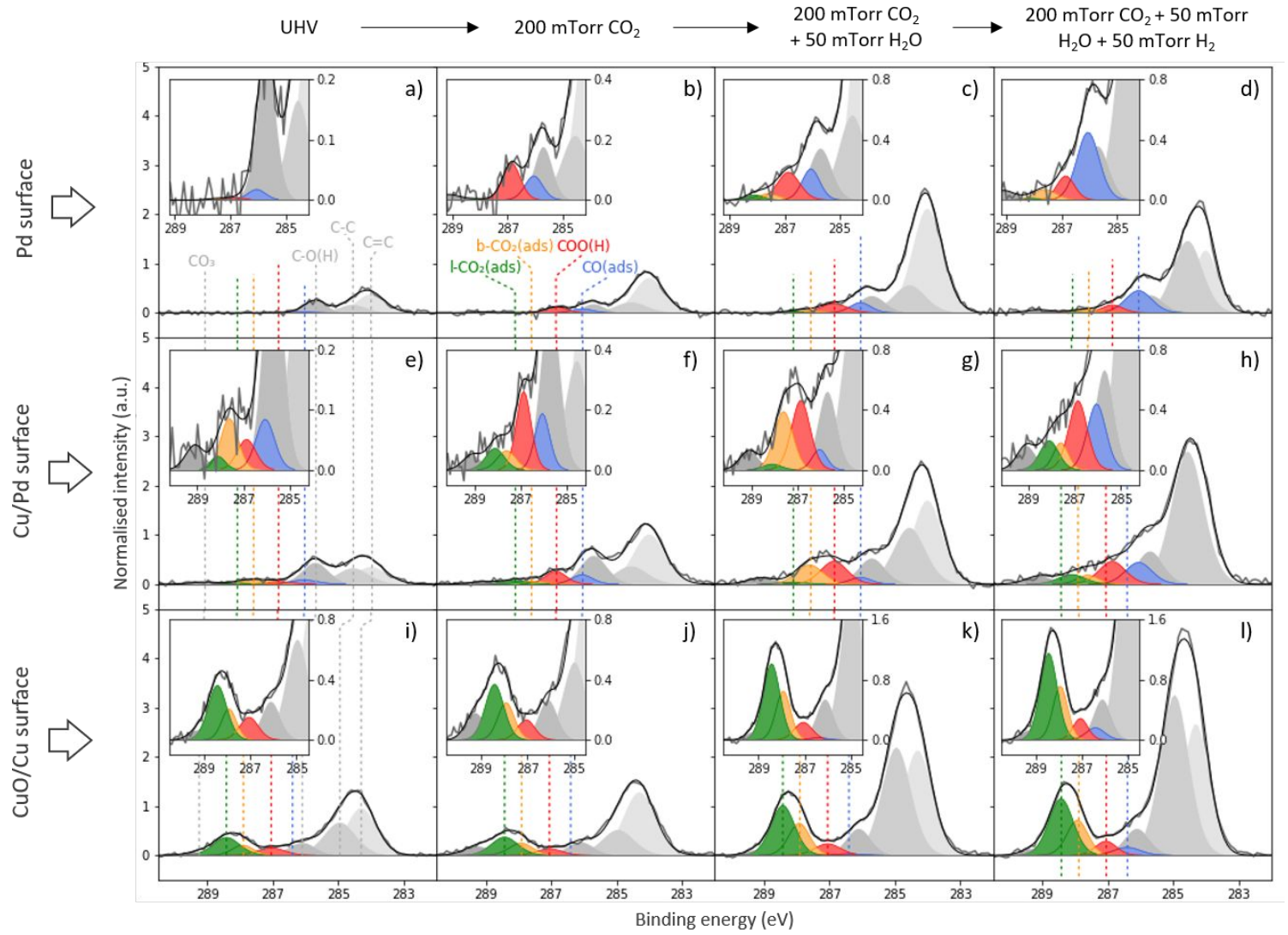

Figure SI-15: C 1s spectra measured at the Pd (a, b, c and d), Cu/Pd (e, f, g and h) and CuO/Cu (I, j k and l) surfaces during the second run of addition of gas. Spectra are initially collected in UHV conditions (a, e and i) before the addition of 200 mTorr CO_2 (b, f and j), 50 mTorr H_2O (c, g and k), 50 mTorr H_2 (d, h and l). The species of interest are l-$CO_{2(ads)}$ (green), b-$CO_{2(ads)}$ (yellow), COOH (red) and $CO_{(ads)}$ (blue).

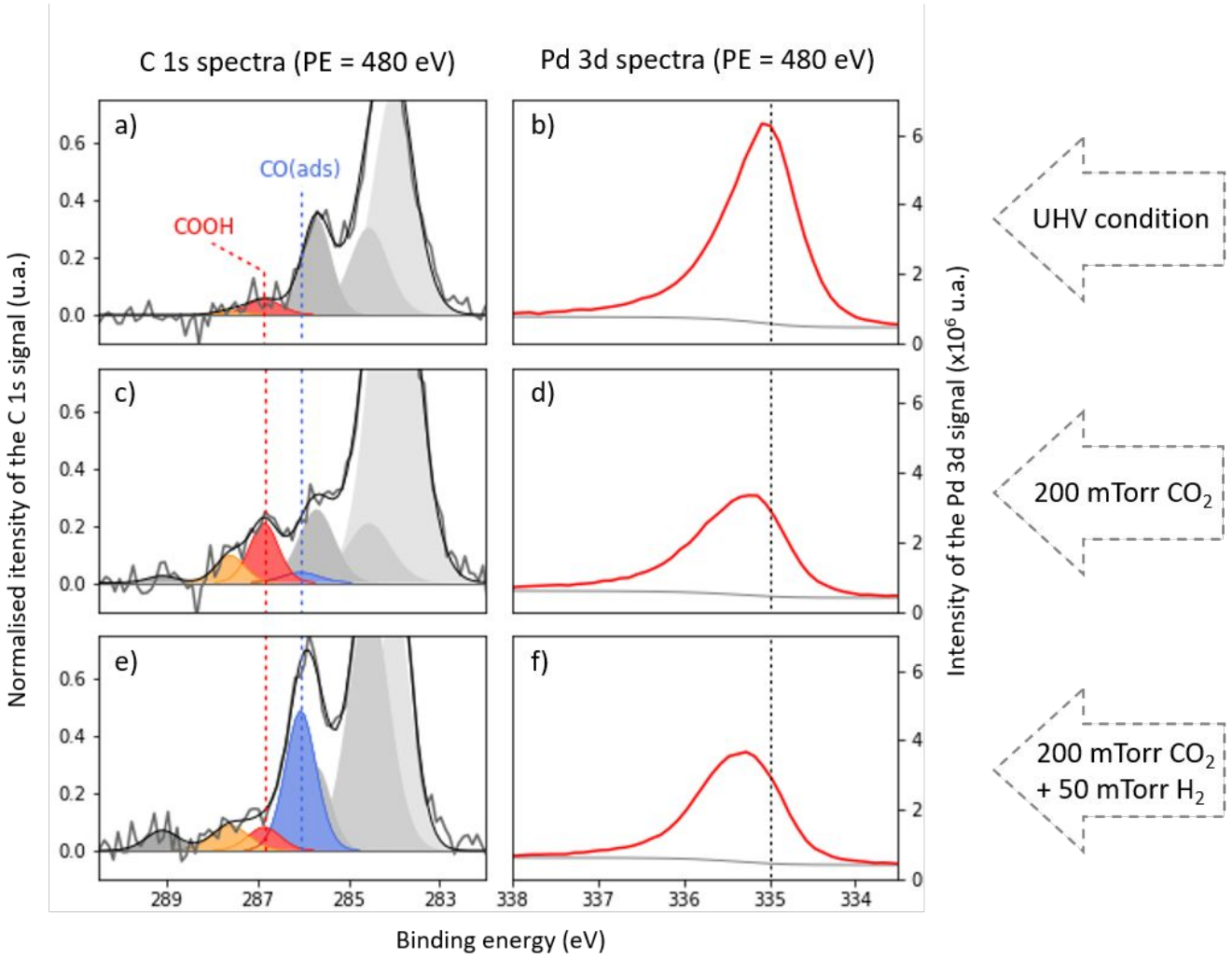

Figure SI-16: Modification of the Pd 3d signal (b, d and f) of collected from the Pd surface as the gaseous condition evolve from UHV (a and b) to CO_2 (c and d) to CO_2 and H_2 (e and f). The C 1s spectra (a, b and c) indicate that COOH appear and $CO_{(ads)}$ adsorbates respectively appear on the surface as the CO_2 and the H_2 are added to the system. The shift of the Pd peak toward the higher binding energy is associated to the adsorption of these species. The dashed line in the spectra b), d) and f) appears at 335.0 eV as a reference mark only.

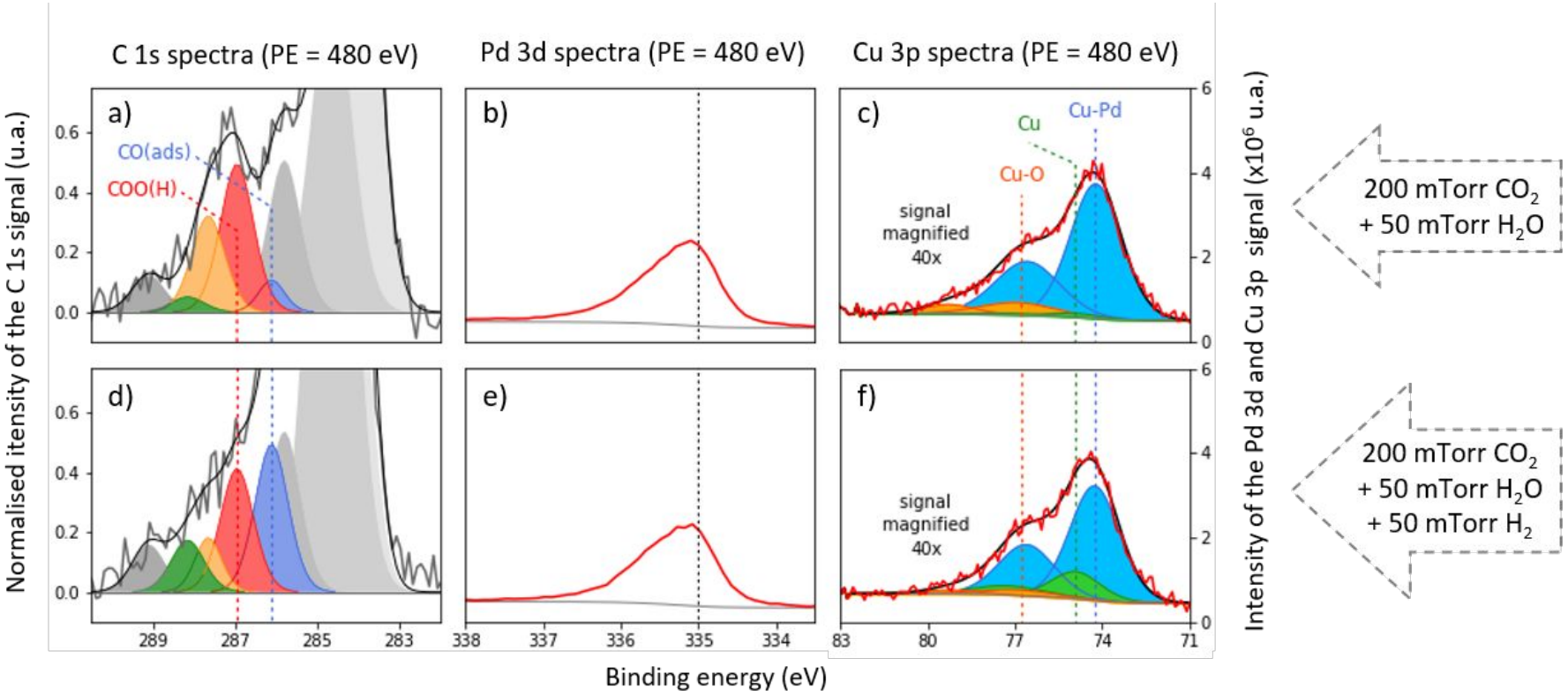

Figure SI-17: Modification of the Cu 3p signal (c and f) collected from the Cu/Pd surface as the gaseous condition change from CO_2 and H_2O (a, b and c) to CO_2, H_2O and H_2 (d, e and f). The C 1s spectra (a and d) indicates that the $CO_{(ads)}$ adsorbates appears on the surface as the H_2 are added to the system. The increase in metallic copper intensity in the Cu 3p spectra is associated to the apparition of this $CO_{(ads)}$ adsorbate. We propose the increase of bulk-like metallic copper at the Cu/Pd surface is the result of the reorganisation of some adatoms of copper from the monolayer. These adatoms would be displaced from their monolayer configuration to the top of the adjacent copper monolayer, hence liberating some site of the substrate for the highly favorable adsorption of $CO_{(ads)}$ on the palladium. The profile of the Pd 3d signal (b and e) not significantly modified by this process of $CO_{(ads)}$ adsorption. The dashed line in b) and e) appears at 335.0 eV as a reference mark only.

Table SI-1: Fitting parameters of the Cu 3p peaks collected at 480 eV

	fitting parameter			comparative value of position (eV)	
specie	peak shape	fwhm (eV)	position (eV)	Ertl *et al.*[3]	Identification
Cu (metallic)	GL(30)	2.0 – 3.0	75.0 – 74.9	74.2	Figure SI-5
Cu-O	GL(30)	2.0 – 3.0	76.9 – 76.6	76.1	Figure SI-6
Cu-Pd	GL(30)	2.0 – 3.0	74.25 – 74.1	-	Figure SI-7

Note : The Cu $3p_{1/2}$ has been restrained to a position systematically 2.35 eV higher than Cu $3p_{3/2}$ peak, an area corresponding to the half of the area of the Cu $3p_{3/2}$ peak. The other fitting parameters for the Cu $3p_{1/2}$ peak are the same than the one used of the Cu $3p_{3/2}$ peak.

Table SI-2: Value of the parameter entering the PAM.

parameters entering calculus of the mean free path λ, Eq. SI-8

atom/ fragment of molecule	Pd	Cu	CO_3	CO_2	COO(H)	CO	-(CHOH)-	$-(CH_2)-$	=(CH)-
atomic number Z	46	29	7.5[i)]	7.33	5.75	7	4	2.67	3,5
number of atom n	-	-	4	3	4	2	4	3	2
photon energy (eV)	480	240	480	480	480	480	480	480	480
kinetic energy KE (eV)	145	165	195	195	195	195	195	195	195

parameters entering the calculus of the normalisation factor N, Eq. SI-6 and SI-7

atom/ fragment of molecule	Pd	Cu	CO_3	CO_2	COO(H)	CO	-(CHOH)-	$-(CH_2)-$	=(CH)-
concentration c (x 10^{28} molecule/m^3)	7.04[ii)]	7.48[iii)]	1.32	1.41	0.80	1.51	1.51	2.20	2.71
molecular volume V (x 10^{-29} m^3)	1.42[iv)]	1.18	7.6[v)]	7.1	12.4	6.6	7.1	4.6	3.7
cross section σ (mBarn)	3.471[vi)]	0.247	0.2988	0.2988	0.2988	0.2988	0.2988	0.2988	0.2988
B (nA)	0.0815	0.019	0.0815	0.0815	0.0815	0.0815	0.0815	0.0815	0.0815

parameter entering the calculus of θ_{Cu}, Eq. SI-15

atom/ fragment of molecule	Pd	Cu	CO_3	CO_2	COO(H)	CO	-(CHOH)-	$-(CH_2)-$	=(CH)-
d (x 10^{-10} m)	-	2.28[vii)]	-	-	-	-	-	-	-

Notes : [i)] The atomic number for the carbon species are the average atomic number of the atoms composing the fragment.

[ii)] The concentration of all atoms/species, except for the Cu, are derived from their molecular volume : $c = {}^{1}/_{V_{molec}}$.

[iii)] The concentration of atoms of Cu in the monolayer is derived from the molar volume of copper in the monolayer: $c_{Cu} = {}^{1}/_{V_{molec\ ML\ Cu}}$. The Cu atoms in the two axes of the monolayer planes are spaced with the distance separating atoms in the Pd bulk. We suppose the configuration in the normal axis is similar to the spacial configuration of the Cu bulk. Accordingly, we approximate the volume of an adatom of Cu on Pd to : $V_{molec\ ML\ Cu} = \sqrt[3]{V_{molec\ bulk\ Cu}} * \sqrt[2/3]{V_{molec\ bulk\ Pd}}$.

[iv] The molecular volume of the metal are derived from the molar volume of their bulk metal adjusted with the Avogadro number : $V_{molec} = V_{molar}/N_A$. The values of molar volume have been retrieved from the CRC Handbook of Chemistry and Physics[4].

[v] The molecular volume of carbon species is derived of the parameter b of the Van der Waals equation of stage of gas. For the gas-like species as CO_2 and CO, the parameter b represents directly the finite volume of the molecules in the gas phase and is taken directly. The molecular volume is derived from the parameter b listed for structurally similar molecules for the other fragments. All the molecular volumes derived from the parameter b are approximative as they do not reflect the real volume of the species adsorbed on metallic surfaces. The values of the parameter b have been retrieved from the CRC Handbook of Chemistry and Physics[5] and adjusted from to their molecular value with the Avogadro number.

[vi] The values of cross section have been retrieved from Yeh and Linday.[2]

[vii] The effective thickness of a single monolayer of copper has been approximated to : $\sqrt[3]{V_{molec\ bulk\ Cu}}$.

Table SI-3: Fitting parameters of the C 1s peaks collected with a photon energy of 480 eV

specie	fitting parameter				comparative value of position (eV)		
	peak shape	fwhm (eV)	Position (eV)		Favaro *et al.*[6] (on metallic or partially oxidized Cu)	Deng *et al.*[7] (on Cu)	Blomberg *et al.*[8] (on Pd)
			on CuO/Cu	on Cu/Pd and Pd			
CO_3	GL(30)	0.75 – 0.95	289.25	289.10	289.4	289.3	-
l-$CO_{2(ads)}$	GL(30)	0.75 – 0.95	288.42	288.10	288.4	288.4 (only 1	-
b-$CO_{2(ads)}$	GL(30)	0.75 – 0.95	287.92	287.60	287.9	peak for CO_2)	-
COO(H)	GL(30)	0.75 – 0.95	287.05	286.85	287.3	287.3	-
$CO_{(ads)}$	GL(30)	0.75 – 0.95	286.40	286.05	-	-	285.9
C-O(H)	GL(30)	0.75 – 0.95	286.10	285.70	286.3	285.2	-
C-C	GL(30)	0.85 – 1.15	284.95	284.55	285.2	284.4	-
C=C	GL(30)	0.85 – 1.15	284.30	284.00	284.5 (graphitic)	284.4	-

References

(1) Walton, J.; Alexander, M. R.; Fairley, N.; Roach, P.; Shard, A. G. Film Thickness Measurement and Contamination Layer Correction for Quantitative XPS. *Surf. Interface Anal.* **2016**, *48*, 164–172.

(2) Yeh, J. J.; Lindau, I. Atomic Subshell Photoionisation Cross Sections and Asymmetry Parameters: 1 < 103. *At. Data Nucl. Data Tables* **1985**, *32*, 1–155.

(3) Ertl, G.; Hierl, R.; Knozinger, H.; Thiele, N.; Urbach, H. P. XPS Study of Copper Aluminate Catalysts. *Appl. Surf. Sci. (1977-1985)* **1980**, *5*, 49–64.

(4) *CRC Handbook of Chemistry and Physics*, 100th ed.; Rumble, J.R., Ed.; CRC Press: Boca Raton, FL, 2019; Section 4, No. 1.

(5) *CRC Handbook of Chemistry and Physics*, 62th ed.; Weast, R.C., Ed.; CRC Press: Boca Raton, FL, 1982; Section D, No. 166.

(6) Favaro, M.; Xiao, H.; Cheng, T.; Goddard, W. A.; Yano, J.; Crumlin, E. J. Subsurface Oxide Plays a Critical Role in CO_2 Activation by Cu (111) Surfaces to Form Chemisorbed CO_2, the First Step in Reduction of CO_2. *Proc. Natl. Acad. Sci. U. S. A.* **2017**, *114*, 6706–6711.

(7) Deng, X.; Verdaguer, A.; Herranz, T.; Weis, C.; Bluhm, H.; Salmeron, M. Surface Chemistry of Cu in the Presence of CO_2 and H_2O. *Langmuir* **2008**, *24*, 9474–9478.

(8) Blomberg, S.; Hoffmann, M. J.; Gustafson, J.; Martin, N. M.; Fernandes, V. R.; Borg, A.; Liu, Z.; Chang, R.; Matera, S.; Reuter, K.; et al. In Situ X-Ray Photoelectron Spectroscopy of Model Catalysts : At the Edge of the Gap. *Phys. Rev. Lett.* **2013**, *110*, 117601/1-117601/5.